Korean J. Chem. Eng., 36(10), 1724-1731 (2019)
DOI: 10.1007/s11814-019-0354-3

pISSN: 0256-1115
eISSN: 1975-7220

Effect of petroleum pitch coating on electrochemical performance of graphite as anode materials

Yoon Ji Jo and Jong Dae Lee†

Department of Chemical Engineering, Chungbuk National University, Cheongju 28644, Korea
(*Received 10 June 2019 • accepted 5 August 2019*)

Abstract−The electrochemical characteristics of artificial graphite coated with petroleum pitch were investigated as anode material in lithium ion batteries. Petroleum pitch with various softening points (SP 150, 200 and 250 °C) was prepared to coat the surface of artificial graphite using tetrahydrofuran as the solvent. Scanning electron microscopy and transmission electron microscopy were used to confirm the coating properties of the prepared anode materials. The electrochemical characteristics of the batteries were investigated by initial charge/discharge, cycle, rate performance, cyclic voltammetry and electrochemical impedance spectroscopy tests in the electrolyte of 1.0 M $LiPF_6$ (EC : DEC= 1 : 1 vol%). With the goal of optimizing the pitch coating process of graphite as an anode material, both the composition ratios of artificial graphite to petroleum pitch and the carbonization temperatures were varied. The best battery anode performance was found to be 10 wt% coated carbon with heat treatment at 1,000 °C on the artificial graphite using petroleum pitch with SP 250 °C. Pitch-derived amorphous carbon coating effectively decreases irreversible capacity and increases the cycle stability. The prepared anode materials have good initial efficiency (92.9%), discharge capacity (343 mAh/g), cycle stability (97%), and rate performance of 10 C/0.1 C (84.1%).

Keywords; Li-ion Batteries, Anode Materials, Petroleum Pitch, Coating, Graphite

INTRODUCTION

Many studies have been developed for Li-ion batteries (LIBs), a promising energy storage device with high power, energy density, and efficiency, as a solution to energy and environmental problems [1,2]; they are thus suitable for electric vehicles and hybrid electric vehicles [3]. Since LIBs being commercialized in the early 1990s, various carbon materials have been applied as anode materials, such as natural graphite (NG), artificial graphite (AG), mesocarbon microbeads, petroleum coke, and petroleum pitch (PP).

Graphite is used as anode material in most LIBs because of its low operating potential, structural stability, reasonable cost, and good cycle life [4]. NG shows relatively high capacity, but it has large irreversible capacity and poor charge/discharge cycle [5]. Although AG's capacity is lower than that of NG, it has excellent cycle characteristics, and research has increased in improving C-rate performance [6]. Carbon coating with graphite was researched to improve the anode performance in LIBs because carbon coating has excellent electric conductivity, high chemical/electrochemical stability and low cost. Carbon as a graphite coating material reduces the irreversible capacity of the initial charge/discharge [7]. Many researchers have identified that pitch coating on AG's surface using various solvents forms a uniform protective film on the surface of graphite, and this pitch coating improves stability by suppressing the reaction between the electrolyte and the graphite. Pitch coating on graphite prevents the formation of complex solid electrolyte interphase (SEI) layer and volume expansion [8-10]. In general, it has been reported that the SEI layer forms on anode materials during the first charge and is mainly determined by electrode surface characteristics such as porosity, surface area, and particle size and shape [11].

There are two ways to coat graphite with carbon: mechanical mixing and coating by solvent. Chemical and thermal vapor decomposition, rotary mixers, and jet mills are used to apply a mechanical coating. Coating methods with solvents such as n-hexane, toluene, and tetrahydrofuran (THF) also use solvent-soluble or insoluble pitch [4,12]. For carbon coating, however, many points have to be clarified, such as the choice of carbon coating precursor, composition ratio, and heat treatment temperature [13].

In this study, AGs coated with PP were prepared to improve initial efficiency, capacity, and stability of the anode material in LIBs. Previous investigators [4,10] used THF as the solvent in the coating process. The physical properties of the samples were investigated by matrix assisted laser desorption ionization-time of flight mass spectrometer (MALDI-TOF-MS), thermogravimetric analysis (TGA) and X-ray diffraction (XRD), and the prepared anode composites were analyzed by scanning electron microscopy (SEM) and transmission electron microscopy (TEM). The electrochemical characteristics of LIBs were investigated by initial charge/discharge, cycle, rate performance, cyclic voltammetry, and electrochemical impedance spectroscopy (EIS) tests in the electrolyte of 1.0 M $LiPF_6$ (EC : DEC=1 : 1 vol%). Anode performance of the resultant pitch-coated graphite in LIBs was evaluated in PP with different softening point (SP). The graphite was coated with the pitch in various composition ratios of AG/PP and at different carbonization temperatures to optimize the anode performance.

†To whom correspondence should be addressed.
E-mail: jdlee@chungbuk.ac.kr

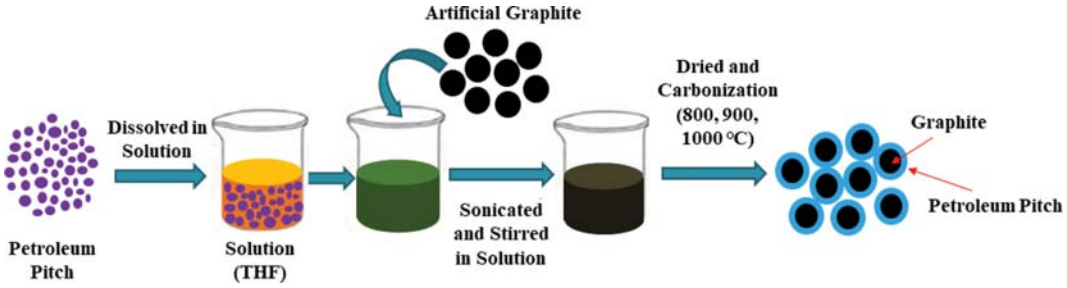

Fig. 1. Schematic diagram for the synthesis of pitch coated graphite.

EXPERIMENTAL

1. Sample Preparation

In the present work, the electrochemical characteristics were investigated of AGs coated with PP as an anode materials. Spherical AG (MTI Korea, Gimhae, South Korea, 19-23 μm) was coated with PP (SP 150, 200 and 250 °C [14]) and THF (OCI Company, Seoul, South Korea, 99.5%) as solvent. Ultra-sonication (60 Hz, 100 W, JEIO TECH, Korea) was used for dispersion, and a hot-plate stirrer (DKSH Technology Sdn Bhd, Selangor Darul, Malaysia) was prepared. Polyvinylidene fluoride (PVdF) was used as the binder for the electrode preparation, and NMP (1-methyl-2-pyrrodidinone, Sigma-Aldrich, St. Louis, MO, USA) was the solvent.

2. Synthesis of Anode Materials

The anode materials were prepared in a range from 50 to 150 mg of PP per 950-850 mg of AGs. PP (SP 150, 200 and 250 °C) was dispersed and dissolved in THF solvent for 10 minutes using ultra-sonication. Then, the AG was added to the solutions in which the pitch was dissolved and dispersed for 30 minutes using ultra-sonication. The mixture was stirred at 150 rpm for 24 hours using a hot plate stirrer to obtain a homogeneous solution that was then transferred into an evaporator and dried at 80 °C. The pitch-coated graphite was heat-treated at 500 °C for 30 min and then carbonized at 1,000 °C for 1 hour under argon flow of 200 cc/min. Fig. 1 shows a schematic diagram of a process for synthesizing AGs coated with PP as an anode material for LIBs.

3. Materials Characterization

The composition of PP fractions was confirmed using MALDI-TOF-MS(Bruker Autoflex Speed TOF/TOF) and 7,7,8,8-tetracyanoquinodimethane (TCNQ, 98%, CAS Number 1518-16-7, Sigma-Aldrich) was used as matrix for the MALDI-TOF analysis. The physical properties of the used PP were analyzed with TGA (D-TGA, SDT 2960, TA Instruments, Champaign, IL, USA) from 25 °C to 1,000 °C in the N_2 atmosphere, and the crystal structure of pitch that was calcined at 500 °C for 30 minutes and at 1,000 °C for 1 hour was analyzed using XRD (Bruker D-5005, Billerica, MA, USA). To investigate the surface change of AGs coated with PP, particle shape was confirmed through SEM (ULTRA PLUS, ZEISS, Oberkochen, Germany). In addition, TEM (Carl Zeiss, Libra 120, 80-120 kV, LaB6 or W) analysis was performed to determine the coating layer thickness of the coated AGs.

4. Electrochemical Measurements

The electrochemical performance of the AGs coated with PP was investigated using CR 2032 coin-type cells assembled in an argon-filled glove box using a lithium metal as the counter and reference electrode. The working electrode consisted of 85 wt% active materials, 10 wt% conductive materials (Super P) and 5 wt% PVdF as binder. After that, the slurry was coated on the copper foil and dried in an oven at 80 °C for 12 hours. The electrode was pressed to a rolling process of thickness (80%) and then dried in a vacuum oven at 120 °C for 2 hours. The electrode was fabricated with a thickness of 40±1 μm, a loading level of 4.0±0.1 mg·cm^{-2}, and a packing density of 1±0.1 g·cm^{-3}.

The electrochemical characteristics of the LIBs prepared using 1.0 M $LiPF_6$ (EC : DEC=1 : 1 vol%) electrolyte were evaluated at a constant temperature of 25 °C using a WBCS 3000 Battery Cycler (WonATech, GyeongGi-Do, Korea). A 25 μm-thick microporous trilayer membrane (Celgard 2400, Celgard, LLC, Charlotte, NC, USA) was used as a separator. Before the Li/graphite half cells' performance was investigated, all cells were aged at 25 °C for 24 h. Subse-

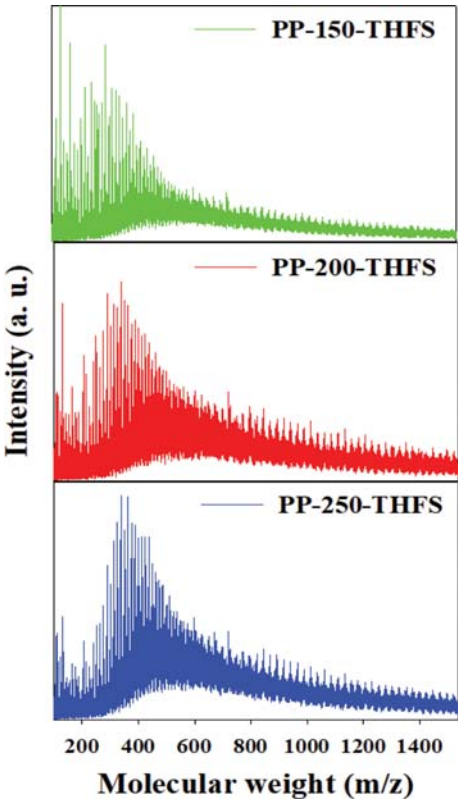

Fig. 2. MALDI-TOF spectrum of the prepared pitch and PFO.

quently, the cells were cycled at room temperature (25 °C) between 0.01 V and 2.5 V for one cycle at 0.1 C using combined constant current/constant voltage (CC/CV) to electrochemically activate the synthesized anode materials. The cycle tests were carried out at 0.1 and 0.2 C with CC/CV and CC/CC, respectively. The rate test was conducted at 0.1, 0.2, 0.5, 1, 2, 5 and 10 C-rate. The cyclic voltammetry test was performed using ZIVE LAB MP2 (WonATech) with a scan rate of 0.1 mV/s at 0-3 V for the electrochemical experiment. The EIS test was carried out using the ZIVE LAB MP2 in the range of 1,000 KHz to 0.01 Hz.

RESULTS AND DISCUSSION

The solubility of the PP with different softening points was characterized to confirm the THF soluble (THFS) and THF insoluble (THFI) properties. The results exhibited that PP-150 had no content of THFI fractions and PP-200 and PP-250 showed content of 4 and 10 wt%, respectively. The composition of PP-THFS fractions was examined using MALDI-TOF analysis, as shown in Fig. 2. The MALDI-TOF analysis results have molecular weight distribution from *m*/*z* 100 to 1536. The molecular weight distribution changed with increased SP. It showed that the peak molecular weight is shifted to the right side as the SP of PP increases. This indicates that PP-250 fraction consisted of larger molecules than those of PP-150 and PP-200.

Fig. 3(a) shows the diagrams of molecular area segments in the MALDI-TOF spectra. Naphthalene was selected as a pseudo-component to divide the area fraction [15]. The area segments were divided as follows: seg 1 (100-128 *m*/*z*), seg 2 (128-256 *m*/*z*), seg 3 (256-384 *m*/*z*), seg 4 (384-512 *m*/*z*), seg 5 (512-640 *m*/*z*), seg 6 (640-768 *m*/*z*), seg 7 (768-896 *m*/*z*), seg 8 (896-1024 *m*/*z*), seg 9 (1024-1152 *m*/*z*), seg 10 (1152-1280 *m*/*z*), seg 11 (1280-1408 *m*/*z*), and seg 12 (1408-1536 *m*/*z*). In the seg 2-3 region, the relative abundance of PP-150-THFS was large, while the relative abundance of PP-250-THFS had a remarkable seg 4-5 region. It is confirmed that PP coated graphite are affected by the molecular weight of PP.

The thermal properties of PP were studied in N_2 atmosphere at a heating rate of 10 °C/min as shown in Fig. 3(b). The carbonization yield was 47.1, 59.0 and 83.5 wt% for PP-150, PP-200 and PP-250, respectively. Differential thermal gravimetry (DTG) is analyzed in Fig. 3(c). The DTG graphs of the PP with various SP show similar peaks from 400 to 500 °C. The peaks are shifted to the right side. Considering these thermal characteristics, controlling the carbonization is related to the peaks [16,17].

Fig. 3(d) shows the crystal structure of the PP based amorphous carbon as the coating materials using XRD. The prepared PP based carbon materials were heat-treated at 500 °C for 30 min and then carbonized at 1,000 °C for 1 hour under argon flow. PP based carbon had an amorphous peak at approximately 5°-30° [18]; 2-theta peaks of (002) were measured at 25.38°, 25.39°, and 25.50° in the samples of PP-150, PP-200 and PP-250 based carbon, respectively. These peaks of (002) were gradually shifted to a higher 2-theta region, depending on the SP. It means that the PP based carbon after the heat-treatment became unorganized carbon such as the

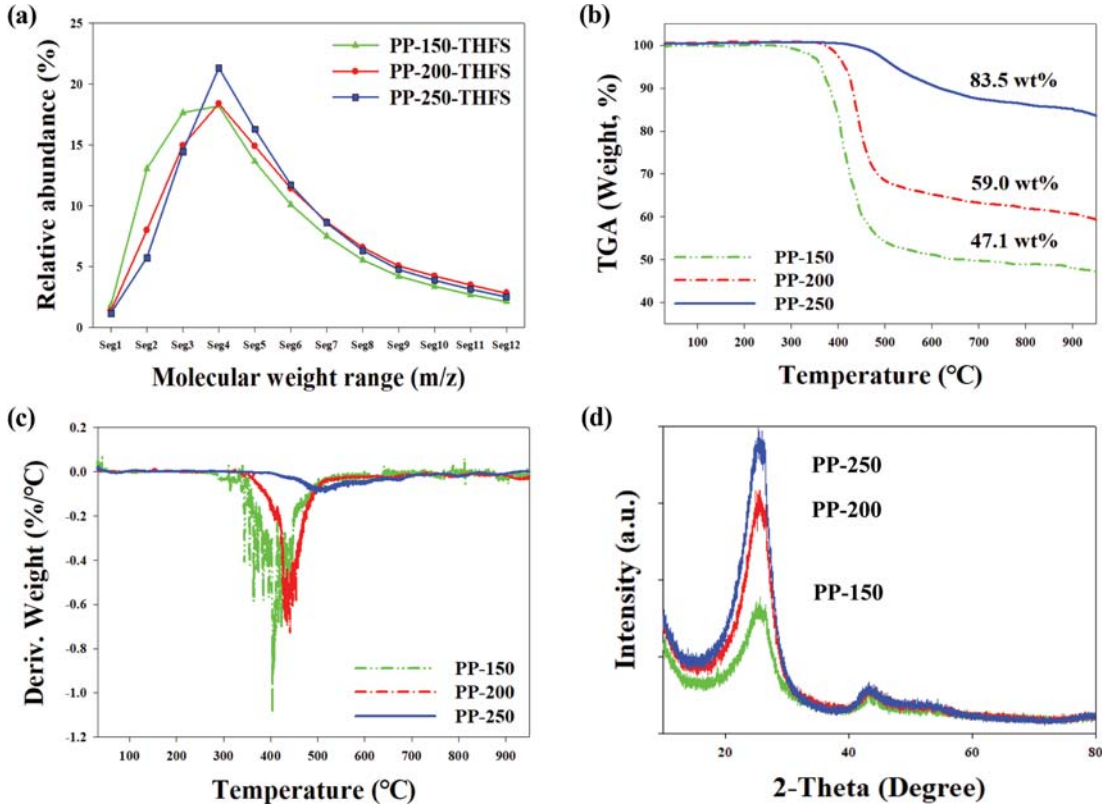

Fig. 3. Physical properties of the used samples: (a) diagram of the molecular weight range of PP-THFS divided by pseudo-component, (b) TGA, (c) DTG of PP and (d) XRD patterns of PP based carbon.

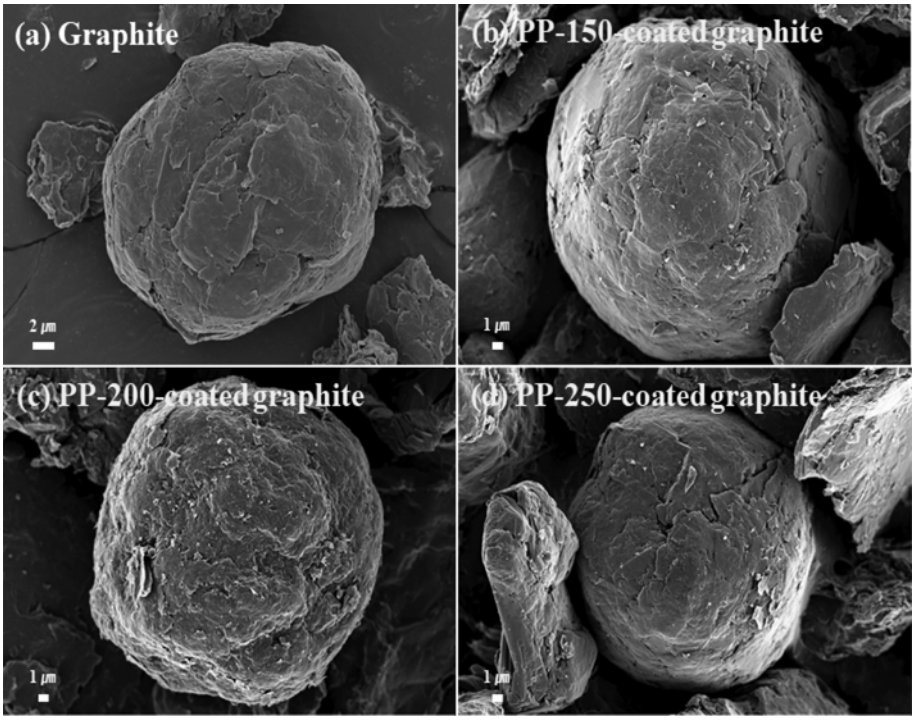

Fig. 4. SEM images of anode materials (a) graphite pristine, (b) PP-150 coated graphite, (c) PP-200 coated graphite and (d) PP-250 coated graphite.

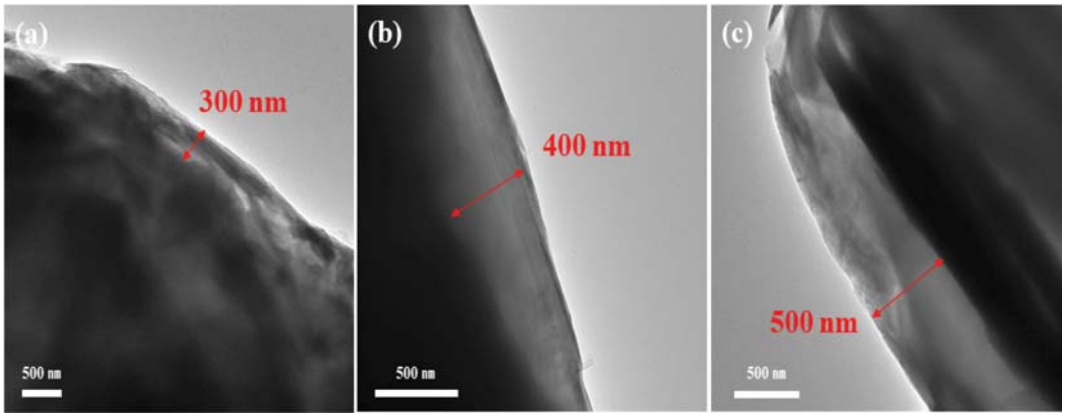

Fig. 5. TEM images of pitch coated graphite (a) PP-150-coated graphite, (b) PP-200-coated graphite and (c) PP-250-coated graphite.

turbostratic structure in which a graphene sheet is randomly stacked [19]. The d_{002} value was 3.35 Å at petroleum pitch of SP 150 °C (PP-150), which is the material of the carbon layer and the d_{002} value of the PP-200 based carbon was 3.36 Å. The PP-250 based carbon had a d_{002} value of 3.39 Å. PP with high SP based carbon had a sharp peak and high peak intensity in the XRD patterns [20].

Surface morphology of the samples observed on SEM is shown by Fig. 4(a)-(d). In Fig. 4(a), many cracks and step-like undulations can be seen on the surface of the pristine AG sphere. SEM observation revealed that carbon coating did not change the spherical shape of the AG particles, as illustrated in Fig. 4; however, some changes on the particle surface took place [21]. After coating, the cracks were properly covered by PP (see Fig. 4(b)-(d)), which acted as a protective layer against the exfoliation of graphite flakes and the penetration of electrolytes into the inner part of the graphite [22]. Also, the morphology of the PP-coated AGs was smoother than that of the pristine AGs, because the coating layer of the pitch complemented the roughness of the AG's surface [23].

In Fig. 5, TEM images illustrate the microstructure and thickness of the pitch coating. In Fig. 5(a)-(c), the AG was coated using PP-150, PP-200 and PP-250, respectively, and the coating thickness was 300-500 nm with PP-150 (300 nm), PP-200 (400 nm), and PP-250 (500 nm). The AG coated with PP-250 had the highest carbonization yield with heat treatment and therefore thicker a SP layer [4]; Yoshio et al. [24] also identified the correlation between carbon coating amount and thickness; coating with 10 wt% carbon

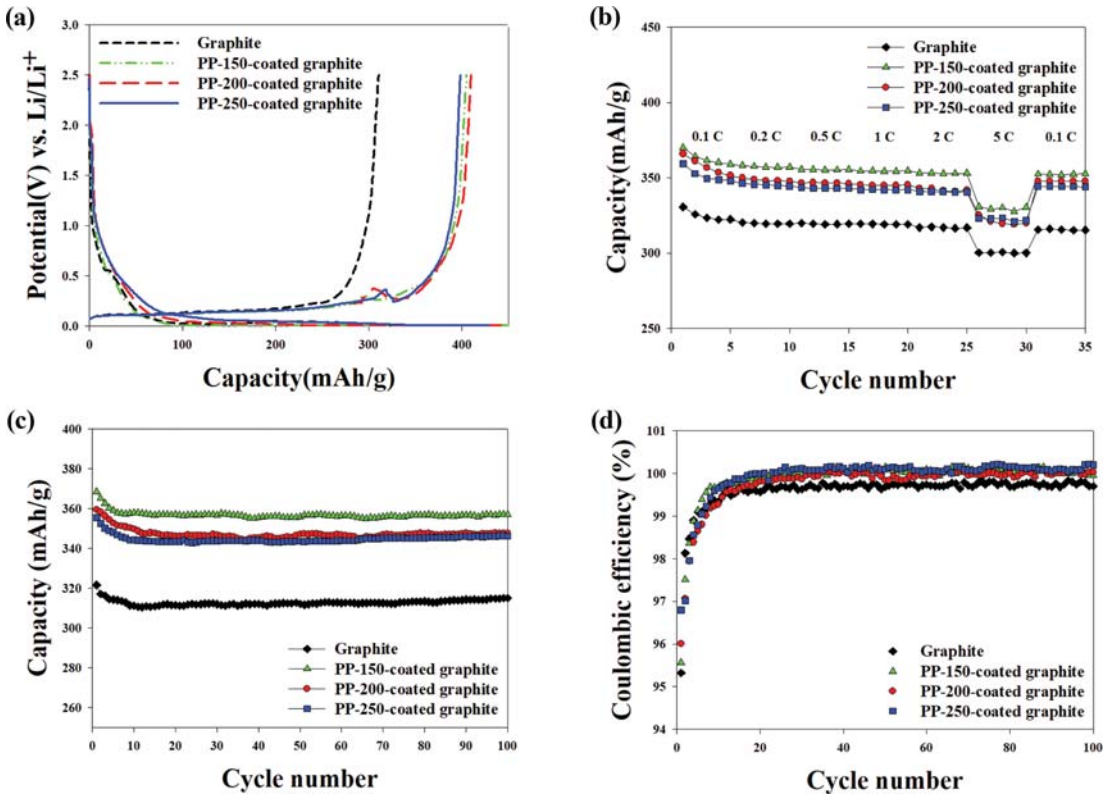

Fig. 6. Electrochemical characterization results for PP-coated graphite: (a) initial charge/discharge curves (b) rate performance, (c) 100-cycle characteristics and (d) coulombic efficiency.

yielded a layer of less than 500 nm.

Fig. 6 shows the electrochemical characterization results for PP-coated graphite. Fig. 6(a) exhibits the first cyclic charge/discharge profiles of graphite coated with PP, which consisted of charge/discharge at 0.1 C between 0.01 and 2.5 V versus Li/Li^+. The first cycle discharge of the PP-coated graphite showed greater capacity (430-469 mAh/g) and initial coulombic efficiency (86-93%) than that of pristine graphite (391 mAh/g, 79.5%), demonstrating that the carbon layer on graphite played an important role in improving the capacity and the initial efficiency; in particular, AGs coated with PP-250 showed initial discharge capacity of 429.1 mAh/g and initial efficiency of 92.9%. The capacity of the PP-250-coated AGs tended to be slightly lower, but cycle stability and initial coulombic efficiency were better than those of the other PP-coated AGs. This coating material showed better results than other carbon materials such as PVA and PVC which indicated the capacity of 355 mAh/g in the first cycle [13]. Peaks at 0.2 V were found in the graph of charge/discharge curves during the first cycle, which was considered to be the peak at which lithium ions showed intercalation/deintercalation on the graphite' surfaces [25].

Fig. 6(b) presents the specific capacity vs. cycle number at various C-rates; the specific capacity gradually decreased with increasing C-rate from 0.1 C to 5 C and increased again when the C-rate was lowered. The PP-150-, PP-200-, and PP-250-coated graphite showed 92.4, 93.3, and 93.7% in 5 C/0.1 C and 96.9, 97.0, and 97.7% in 0.1 C/0.1 C, respectively when the pristine graphite indicated 92.1% in 5 C/0.1 C and 96.7 in 0.1 C/0.1 C. It was considered that the PP-250 afforded better homogeneous amorphous carbon coating on the graphite surfaces than that of other PP coatings, which enhanced the rate capability of PP-250-coated graphite.

After the first CC/CV charge/discharge profiles were completed, Fig. 6(c) displays the cycle performance of the graphite coated with PP-derived carbon with SP of 150, 200, and 250 °C; the pristine and PP-coated graphite showed stable cycle performance during 100 cycles using charge/discharge rates of 0.1 C. The discharge capacity of the pristine graphite and the PP-150-, PP-200-, and PP-250-coated AG composite electrodes was 322, 369, 359, and 355 mAh/g in the first cycle and remained at 307, 357, 348, and 346 mAh/g after 100 cycles, respectively. The PP-coated AGs showed better capacity retention (96-98%) than the original AGs without pitch coating (94%) from the 2nd to 100th cycles; the slight decrease in capacity during 100 cycles was attributed to electrolyte decomposition. To verify the irreversible capacity loss of the electrodes, coulombic efficiency profiles were developed as shown in Fig. 6(d); the figure confirms that after the SEI layer formed during first cycle, high coulombic efficiency was obtained. The graph shown in Fig. 6(d) is the coulombic efficiency of the cycle data in Fig. 5(c).

Fig. 7 shows the cyclic voltammograms of the graphite and PP-coated graphite for five cycles. During electrochemical activation, CC/CV charging/discharging was performed using cut-off voltages and scan rates of 0.01-3.0 V (vs. Li/Li^+) and 0.1 mV/s, respectively. The increase in redox currents with successive cycling indicated that there was electrochemical activation during lithiation/delithiation. One broad reduction peak located at 0.65 V disappeared from

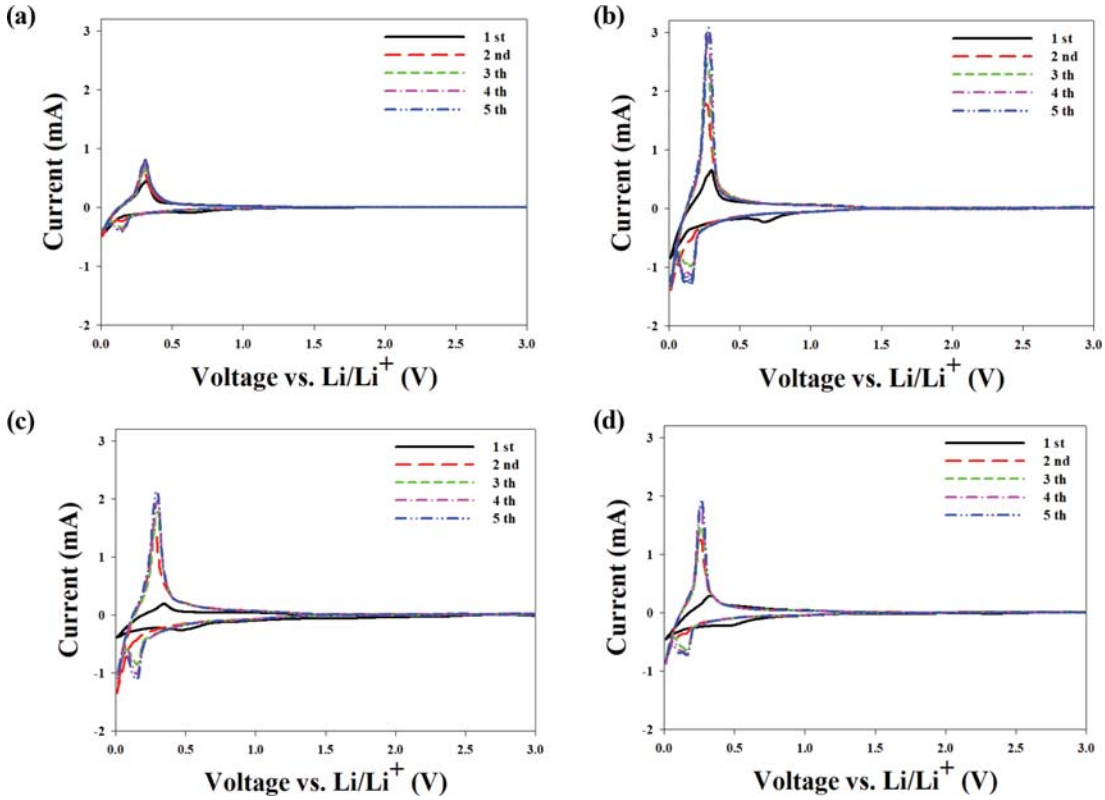

Fig. 7. Cyclic voltammetry curves of (a) pristine artificial graphite and graphite coated with (b) PP-150, (c) PP-200 and (d) PP-250.

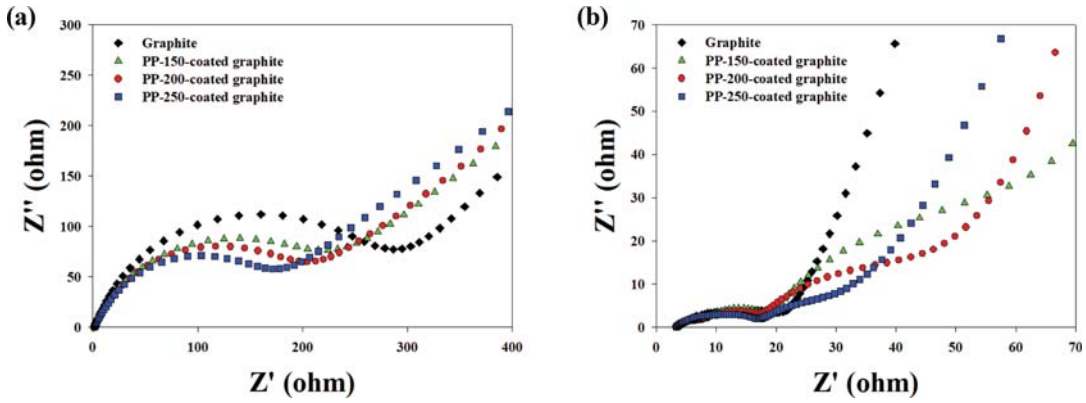

Fig. 8. Nyquist plots of PP-coated graphite (a) before charge/discharge cycling and (b) after the 100 cycles.

the second cycle; the reduction peak could be attributed to the formation of a SEI layer on the surface of the electrode, which improved the reversibility of lithium ion insertion and extraction [26]. Lithium ions were adsorbed on low-crystalline carbon at 1.2 V, and researchers predicted that lithium was inserted and extracted between graphite layers at 0.2 V of graphite [27]. The comparison between the CV curves of the pristine graphite and the graphite coated with PP-150, PP-200, and PP-250 revealed that the potential difference in redox peaks decreased after PP coating; this meant that the electrode polarization decreased after the PP coating, which improved the performance of anode materials [21]. The area of the first cycle for bare graphite was smaller than that for the PP-coated graphite in CV curve. This phenomenon was consistent with the tendency to increase capacity [28].

EIS is a useful way to evaluate the electron conductivity and Li^+ diffusion rate of anode materials. As shown in Fig. 8, the pristine and synthesized graphite demonstrated one semicircle at high frequency and a straight sloping line at low frequency [29,30]. PP as a graphite coating material can supply fast electrons and be permeable for Li^+ ions from the surrounding electrolyte solution. This approach ensures the effective ambipolar diffusion of Li^+ and e^- into/out of active particles. The Nyquist plot confirmed that the resistance decreased as the SP of PP increased before charge/discharge cycling [31]. Moreover, the PP-250 coated graphite showed

Table 1. Electrochemical properties of composition ratios with artificial graphite and pitch

	Graphite	PP-250 coated graphite 1	PP-250 coated graphite 2	PP-250 coated graphite 3
Graphite : Pitch (wt%)	100 : 0	95 : 5	90 : 10	85 : 15
Ist Irreversible capacity (mAh/g)	89	36	29	27
Capacity (mAh/g)	329	348	361	374
Coulombic efficiency at the 30th cycle (%)	97	97	99	98

lower charge transfer resistances than other PP coated graphite after the repeated cycling, indicating the effective action of PP-250 to boost the electron transfer and electrochemical lithiation/delithiation.

Table 1 lists electrochemical properties of the PP-250-coated graphite. Cycle tests were performed at 0.2 C to investigate the coating conditions according to the composition ratio of graphite/PP in anode materials,. The pristine graphite showed initial irreversible capacity of 89 mAh/g; capacities for the anode material synthesized at the weight ratios of graphite : PP=95 : 5, 90 : 10, and 85 : 15) were significantly lower, 36, 29, and 27 mAh/g, respectively. Because the pitch amorphous coating layer compensated for the artificial graphite surface, the irreversible capacity loss was improved with the formation of the initial SEI layer. The pristine graphite showed a capacity of 329 mAh/g, and the PP-250-coated graphite at the above weight ratios had capacities of 348-374 mAh/g. It was noted that the amorphous carbon coating enhanced the specific capacity of the graphite.

The rate capabilities are shown in Fig. 9 of the graphite coated with PP-derived carbon at different carbonization temperatures from 800 to 1,000 °C. The PP-250-coated graphite used in the anode materials had the graphite : PP ratio of 90 : 10 wt/wt%, and at 800 °C exhibited capacity recovery rates of 83.4% at 10 C/0.1 C and 96.8% at 0.1 C/0.1 C. The PP-250-coated graphite heated at 900 °C showed capacity retention rates of 83.8% at 10 C/0.1 C and 97.6% at 0.1 C/0.1 C, and at 1,000 °C, the rates were 84.1% for 10 C/0.1 C and 98.1% for 0.1 C/0.1 C. The capacity decreased but the retention stability at high C-rate increased as the carbonization temperature increased.

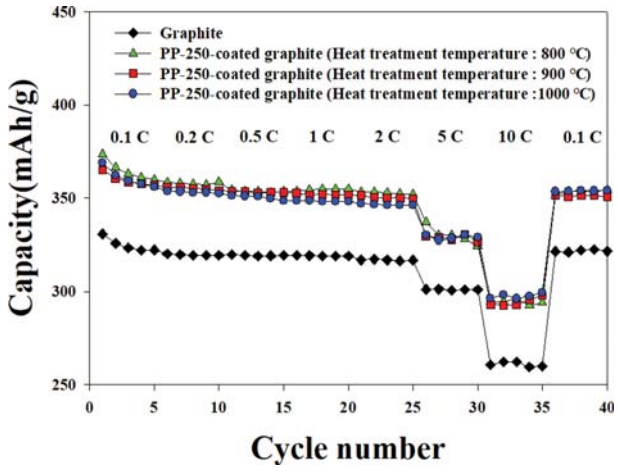

Fig. 9. Rate performance of PP-250-coated graphite at different heat treatment temperature.

CONCLUSIONS

Petroleum pitch coating on sphere graphite was studied to improve initial efficiency and structural stability for anodes. Pitch with various softening points was prepared to coat the surfaces of artificial graphite using THF as solvent. The pitch-coated graphite showed improved initial efficiency due to its superior surface morphology. The characteristics of anode materials were also investigated at various composition ratios, and carbonization increased the specific capacity and cycle stability. From the experimental results, the graphite coated with petroleum pitch at SP 250 °C showed coating thickness of 500 nm at the graphite:pitch composition of 90 : 10 wt/wt% and carbonization temperature of 1,000 °C. The prepared anode materials have excellent electrochemical characteristics: initial efficiency (92.9%), discharge capacity (343 mAh/g), cycle stability (97%), and rate performance (84.1% at 10 C/0.1 C).

ACKNOWLEDGEMENTS

This research was supported by Korea Evaluation Institute of Industrial Technology (KEIT) through the Carbon Cluster Construction project [10083621, Development of preparation technology in petroleum-based artificial graphite anode] funded by the Ministry of Trade, Industry & Energy (MOTIE, Korea).

REFERENCES

1. H. S. Ko, J. H. Kim, J. Wang and J. D. Lee, *J. Power Sources*, **372**, 107 (2017).
2. H. S. Ko, H. W. Park and J. D. Lee, *Korean Chem. Eng. Res.*, **56**(5), 718 (2018).
3. S. H. Lee and J. D. Lee, *Korean Chem. Eng. Res.*, **56**(4), 561 (2018).
4. Y. J. Han, J. Kim, J. S. Yeo, J. C. An, I. P. Hong, K. Nakabayashi, J. Miyawaki, J. D. Jung and S. H. Yoon, *CARBON*, **94**, 432 (2015).
5. S. H. Liu, Z. Ying, Z. M. Wang, F. Li, S. Bai, L. Wen and H. M. Chemg, *NEW CARBON MATERIALS*, **23**(1), 30 (2008).
6. N. Ohta, K. Nagaoka, Z. Hoshi, S. Bitoh and M. Inagaki, *J. Power Sources*, **194**, 985 (2009).
7. H. Li and H. Zhou, *Chem. Commun.*, **48**, 1201 (2012).
8. B. H. Kim, J. H. Kim, J. G. Kim, M. J. Bae, J. S. Im, C. W. Lee and S. Kim, *J. Ind. Eng. Chem.*, **41**, 1 (2016).
9. H. S. Ko, J. E. Choi and J. D. Lee, *Appl. Chem. Eng.*, **25**(6), 592 (2014).
10. Y. J. Jo and J. D. Lee, *Korean Chem. Eng. Res.*, **57**(1), 5 (2019).
11. M. L. Lee, Y. H. Li, S. C. Liao, J. M. Chen, J. W. Yeh and H. C. Shih, *Electrochim. Acta*, **112**, 529 (2013).
12. S. H. Yoon, H. J. Kim and S. M. Oh, *J. Power Sources*, **94**, 68 (2001).

13. H. Nozakia, K. Nagaoka, K. Hoshi, N. Ohta and M. Inagaki, *J. Power Sources*, **194**, 486 (2009).
14. J. G. Kim, J. H. Kim, J. S. Im, Y. S. Lee and T. S. Bae, *J. Ind. Eng. Chem.*, **62**, 176 (2018).
15. S. W. Seo, Y. J. Choi, J. H. Kim, J. H. Cho, Y. S. Lee and J. S. Im, *Carbon Letters*, **29**, 385 (2019).
16. H. L. Zhang, F. Li, C. Liu and H. M. Cheng, *J. Phys. Chem. C*, **112**, 7767 (2008).
17. Y. J. Han, J. U. Hwang, K. S. Kim, J. H. Kim, J. D. Lee and J. S. Im, *J. Ind. Eng. Chem.*, **73**, 241 (2019).
18. J. G. Kim, J. H. Kim, B. J. Song, C. W. Lee and J. S. Im, *J. Ind. Eng. Chem.*, **36**, 293 (2016).
19. A. Mabuchi, *TANSO*, **65**, 298 (1994).
20. B. H. Kim, J. H. Kim, J. G. Kim, J. S. Im, C. W. Lee and S. Kim, *J. Ind. Eng. Chem.*, **45**, 99 (2017).
21. C. Wang, H. Zhao, J. Wang, J. Wang and P. Lv, *Ionics*, **19**, 221 (2013).
22. H. L. Zhang, S. H. Liu, F. Li, S. Bai, C. Li, J. Tan and H. M. Cheng, *Carbon*, **44**, 2212 (2006).
23. C. Wan, H. Li, M. Wu and C. Zhao, *J. Appl. Electrochem.*, **39**, 1081 (2009).
24. M. Yosio, H. Wang, K. Fukuda, T. Umeno, T. Abe and Z. Ogumi, *J. Mater. Chem.*, **14**, 1754 (2004).
25. J. R. Dahn, *Phys. Rev. B*, **44**, 9170 (1990).
26. L. Gan, H. Guo, Z. Wang, X. Li, W. Peng, J. Wang, S. Huang and M. Su, *Electrochim. Acta*, **104**, 117 (2013).
27. H. Wang and M. Yoshio, *J. Power Sources*, **93**, 123 (2001).
28. W. Ma, Y. Zhuang, Y. Deng, X. Song, X. Zuo, X. Xiao and J. Nan, *J. Power Sources*, **376**, 91 (2018).
29. J. Xie, L. Tong, L. Su, Y. Xu, L. Wang and Y. Wang, *J. Power Sources*, **342**, 529 (2017).
30. D. Aurbacha, B. Markovskya, I. Weissmana, E. Levia and Y. Ein-Eli, *Electrochim. Acta*, **45**, 67 (1999).
31. M. Gaberscek, R. Dominko and J. Jamnik, *Electrochem. Commun.*, **9**, 2778 (2007).